Stapp Car Crash Journal, Vol. 48 (November 2004), pp.

In Vivo Cervical Facet Capsule Distraction: Mechanical Implications for Whiplash & Neck Pain

Kathryn E. Lee, Martin B. Davis, Roanne M. Mejilla, and Beth A. Winkelstein
Department of Bioengineering
University of Pennsylvania
120 Hayden Hall, 3320 Smith Walk
Philadelphia, Pennsylvania, 19104-6392
winkelst@seas.upenn.edu
(phone) 215-573-4589; (fax) 215-573-2071

ABSTRACT – While extensive research points to mechanical injury of the cervical facet joint as a mechanism of whiplash injury, findings remain speculative regarding its potential for causing pain. The purpose of this study was to examine the relationship between facet joint distraction, capsular ligament strain, cellular nociceptive responses, and pain. A novel rat model of *in vivo* facet joint injury was used to impose C6/C7 joint distraction in separate studies of subcatastrophic and physiologic vertebral distraction, as well as sham procedures. A common clinical measure of behavioral hypersensitivity (allodynia) was measured for 14 days after injury, as quantification of resulting pain symptoms. Also, on day 14, spinal activation of microglia and astrocytes was quantified to examine the potential role of glial activation as a physiologic mechanism of facet-mediated painful injury. Vertebral distractions of 0.90±0.53 mm across the rat facet joint reliably produced symptoms of persistent pain. Allodynia results showed immediate and sustained behavioral sensitivity following subcatastrophic vertebral distractions; pain symptoms were significantly greater ($p<0.008$) than those for other injury groups. Further, spinal astrocytic activation was also greater ($p=0.049$) for subcatastrophic injuries compared to lower distraction magnitudes. The mean maximum principal strain in the capsular ligament for joint distractions of 0.57±0.11 mm was 27.7±11.9%. Findings suggest that facet capsule strains comparable to those previously reported for whiplash kinematics and subcatastrophic failures of this ligament have the potential to produce pain symptoms and alter one element of nociception. Results further suggest that a mechanical threshold likely exists for painful joint distraction, providing behavioral and physiologic evidence of the cervical facet joint's mechanical injury as a source of neck pain.

KEYWORDS – Facet Joint; Biomechanics; Whiplash; Pain; Strain; Neck

INTRODUCTION

Whiplash injuries and their associated disorders are a widespread problem in today's society, with a high incidence and large economic costs (Barnsley et al. 1994; Freeman et al. 1999). Neck injuries comprise 30% of all traffic-related visits to US emergency rooms (Quinlan et al. 2004). Neck pain constitutes one-third of all chronic pain cases, making painful neck injury a tremendous problem in today's society. As many as 42% of whiplash injuries become chronic, with neck pain persisting in as many as 10% of those cases (Barnsley et al. 1994). The costs associated with these injuries are staggering, with over $29 billion spent annually on whiplash injuries (Freeman et al. 1999). However, despite the high incidence and economic cost of whiplash-related neck pain and its symptoms, little remains known about the injury mechanisms initiating these painful syndromes and the physiologic sequelae responsible for the persistence of neck pain.

Pain is defined as an unpleasant sensory and emotional experience associated with actual or potential tissue damage, or described in terms of such damage (Merskey and Bogduk 1994). The set of physiological processes responsible for pain signaling and perception is collectively described as nociception. Normally, specialized nociceptors receive noxious stimuli and transmit information about these stimuli to the central nervous system (CNS) via the Aδ and C nerve fibers. Aδ fibers are thinly myelinated fibers (1-5 μm in diameter) that have fast conduction velocities for transmitting information about the initiation of pain sensation, while C fibers are unmyelinated fibers (0.5-2 μm in diameter) with slower conduction velocities, which transmit information about ongoing pain sensation

(Guyton and Hall 1996). Typically, following painful injury, chemical substances are released, both in the injured tissue and the CNS, which may serve as modulators of pain responses (Cavanaugh 2000). These substances include such neuropeptides as substance P and calcitonin gene-related peptide (CGRP), both of which have been strongly implicated in pain transmission and its modulation (Cavanaugh 2000; Doyle and Hunt 1998) (see later section). In addition, a host of other electrophysiological and neurochemical changes also contribute to sustained pain. Ultimately, these and other physiologic responses contribute to nociceptive cascades and can lead to pain symptoms. As such, injury and pain are related by a complex network of chemical changes and signaling events, which are manifest clinically in symptoms. Understanding these mechanisms can potentially provide context for preventing these injuries and treating their symptoms.

Neck Pain and Cervical Facet Joint

While clinical, epidemiological, and biomechanical studies have implicated many different anatomical structures in the neck in whiplash-related pain (April and Bogduk 1992; Barnsley et al. 1993, 1994; Bogduk and Marsland 1988; Lord et al. 1996), the cervical facet joint has been identified as a likely candidate for pain generation due to its mechanical loading during these injuries. In clinical studies of neck pain patients, facet joint provocation and/or anesthetic blocks were used to identify the cervical facet joint as the site of neck pain in 25-62% of cases (April and Bogduk 1992; Barnsley et al. 1994). Further, anesthetic nerve blocks of painful facet joints offered relief to patients with both whiplash-induced and idiopathic neck pain, further suggesting a potential for this joint as a pain source (Barnsley et al. 1993; Bogduk and Marsland 1998; Lord et al. 1996). Clinical and biomechanical studies have suggested that the lower cervical spine is most susceptible to injury (April and Bogduk 1992; Cusick et al. 2001; Grauer et al. 1997; Ito et al. 2004; Kaneoka et al. 1999; Ono et al. 1997; Panjabi et al. 2004), with C6/C7 sustaining the greatest strains during simulated whiplash accelerations (Pearson et al. 2004). While studies suggest the involvement of facet joint injury in neck pain, data remain inferential regarding this joint's ability to generate pain symptoms following injury.

Neuroanatomic & Neurophysiologic Studies. Histologic studies have identified both mechanoreceptors and nociceptors throughout the structures of the facet joint, including its facet capsule. The inner and outer layers of the facet capsule, as well as synovial and subsynovial tissues in rabbit, rat, and human tissue have been histologically demonstrated to contain group I, II, III and IV nerve fibers (Cavanaugh et al. 1996, 1989; McLain 1994; Inami et al. 2001). The presence of group III and IV (Aδ and C) fibers is particularly relevant to pain, as these nociceptive fibers are responsible for pain transmission (Cavanaugh et al. 1996). Immunohistochemical studies of these same animal species have demonstrated nociceptors in cervical and lumbar facet joints reactive for substance P and CGRP (Beaman et al. 1993; El-Bohy et al. 1988; Giles and Harvey 1987; Inami et al. 2001; Kallakuri et al. 2004; Ohtori et al. 2003), neuropeptides particularly relevant to pain signaling. Electrophysiologic studies in the rabbit and rat have demonstrated that nerve fibers innervating the lumbar facet capsule can be activated by compression and tension loading of the L3-L7 spinal region (Avramov et al. 1992; Cavanaugh et al. 1989, 1996). In addition, these fibers required a high intensity stimulus for activation, which is a characteristic of nociceptors. Once activated, fibers demonstrated slow conduction velocities, typical of unmyelinated nociceptors (C fibers). The presence and behavior of these nociceptive fibers during joint loading indicates neural input from the facet joint is likely important for pain sensation throughout the spine. Despite the strong evidence supporting a role for the facet joint and its capsule in whiplash injury and neck pain, no studies have specifically investigated the role of facet joint loading in generating neck pain symptoms.

Biomechanical Investigations. Biomechanical studies of human cadavers provide additional support for a mechanical role of the cervical facet joint in whiplash injury. Studies using high-speed imaging techniques during whiplash injury simulations of volunteers and cadavers document altered kinematics of the lower cervical spine (Grauer et al. 1997; Ito et al. 2004; Kaneoka et al. 1999; Luan et al. 2000; Ono et al. 1997; Pearson et al. 2004; Yoganandan et al. 2002), which can lead to facet joint impingement, synovial fold pinching, and facet capsule stretch (Kaneoka et al. 1999; Ono et al. 1997; Panjabi et al. 1998a,b; Pearson et al. 2004; Yoganandan et al. 1998, 2001, 2002). Also, in mechanical studies involving cadaveric head-neck specimens and cervical spine motion segments in flexion, extension, and combined bending and shear, the facet capsule has been reported to be at risk for *subcatastrophic* injury for vertebral motions occurring during these low-velocity impacts (Pearson et al. 2004; Siegmund et al. 2001; Winkelstein et al. 1999, 2000). While these studies suggest that subcatastrophic capsule injury may present a mechanism for nociceptor

activation, it remains to be seen whether such injuries contribute to painful symptoms.

Cervical Facet Capsule Ligament Mechanics. Many studies have examined the cervical facet capsule specifically for its risk of mechanical injury. Kaneoka et al. (1999) demonstrated altered facet joint motion during human volunteer studies of rear-impact collision with differential kinematics between upper and lower cervical spine regions. Panjabi et al. (1998b) estimated linear capsular ligament strains using transducers inserted in the articular facets to quantify displacements across the C6/C7 joint. For 6.5g accelerations of cadaveric head-neck specimens, C6/C7 capsular strains reached a peak of 29.5±25.7%. However, for these same specimens, the maximum C6/C7 capsule strain was 6.2±5.6% for flexion-extension moments producing normal ranges of motion, suggesting capsular elongation in whiplash as a potential mechanism of injury. More recent work by that group (Pearson et al. 2004) has further substantiated the C6/C7 joint as experiencing the greatest strains during simulated accelerations. For 8g accelerations, Pearson et al. (2004) reported the maximum C6/C7 strain produced by facet joint sliding and separation was 39.9±26.3%, consistent with earlier work of Panjabi et al. (1998b). Yoganandan et al. (2002) quantified relative facet motion (local sliding and compression) for human cadaveric head-neck whiplash simulations and demonstrated mean peak sliding motions in the anterior and posterior joint regions of 2.76±0.78mm and 1.94±0.98mm, respectively; mean peak compression motions in anterior and posterior regions of 2.02±0.65mm and 2.84±0.47mm, respectively. These studies provide evidence that whiplash kinematics alter strains across the bony surfaces of the facet joint and further hypothesize this as a mechanism contributing to painful capsule injury.

While experimental findings have examined strains across the facet joint as a mechanism of whiplash injury, more recent work has focused specifically on closer examination of the cervical facet capsule strain field. For vertebral bending motions matching human volunteer whiplash kinematics, full-field capsular strains have been quantified for cervical motion segments. For these joint kinematics, maximum principal strains were found to be directed across the joint (Winkelstein et al. 1999, 2000), in a direction perpendicular to the joint articulation. While not sustaining any gross capsule injury during these vertebral kinematics, maximum principal strains reached as high as 23.0±4.4%. These strains were not significantly different from those capsular strains (64.6±73.8%) produced at the first ("subcatastrophic") failure during tensile testing of the isolated capsule. Despite the 2.5-fold difference in strains reported for those conditions, the lack of statistical difference due to high variation in subcatastrophic strains led the authors to suggest that whiplash-like bending of the facet joint can produce maximum capsular strains that are similar to those produced during pure tension. Likewise, Siegmund et al. (2001) also documented the likelihood of subcatastrophic failures in combined shear loading during whiplash kinematics, with the capsule sustaining strains of 35.0±21.0%. The broad collection of full spine and motion segment studies suggests a capsular strain threshold for whiplash-related injury, potentially producing neck pain. While these studies provided mechanical bases for whiplash pain and a potentially painful facet capsule subcatastrophic injury, they did not provide physiologic context for those subcatastrophic injuries.

Considering all data from biomechanical testing using human volunteers, head-neck preparations and motion segments, it is possible that a critical distraction of the facet joint may be required for its painful capsular injury. It is hypothesized that such a distraction threshold may initiate nociception and/or pain symptoms. As such, this study examines a range of vertebral distractions, which is inclusive of those distractions producing subcatastrophic C6/C7 capsular strains, as noted in human cadaveric whiplash studies (Siegmund et al. 2001; Winkelstein et al. 2000). Using human capsule dimensions and displacement responses under tensile loading (Winkelstein 1999; Winkelstein et al. 1999), geometric scaling between the human and rat species defined vertebral distraction ranges for the present study. Accordingly, vertebral distractions in the rat (0.9 mm = *SV*), scaled to be equivalent to joint distractions for human subcatastrophic failures, are examined for their potential to induce pain symptoms. Moreover, to evaluate whether joint distraction below these levels initiates any nociceptive or symptom outcomes, vertebral distractions sufficiently below (<10%) the *SV* magnitude are also examined (0.1 mm = *PV*). This study examines these two categories of vertebral distraction *in vivo*, in the context of pain behavioral outcomes and one indicator of nociception for insight into facet-mediated neck pain.

Spinal Cord Mechanisms of Nociception

Nociceptive responses leading to pain occur both in the peripheral nervous system (PNS) at the injury site

and also in the central nervous system (CNS). The facet joint is dually innervated by the medial branches of the dorsal root of the spinal nerves from levels superior and inferior to each joint (Bogduk and Marsland 1988). The afferent fibers of these dorsal roots carry sensory information to the spinal cord and terminate on neurons in the lamina I region of the dorsal horn. As the site of analysis and integration of sensory information, the CNS (spinal cord and brain) contains both neurons and glial cells. Glia constitute over 70% of the total cell population in the CNS and serve as supporting cells that help maintain the normal survival, function, and signaling abilities of neurons (DeLeo and Yezierski 2001). Two types of glial cells, microglia and astrocytes, participate in CNS immune reactions and have been shown to play a role in pain (Watkins et al. 2001). Proliferation and activation of glial cells are hallmarks of PNS and CNS responses to neural injury (Hill-Felberg et al. 1999; Liu et al. 2000; Meon and Landerholm 1994; Piehl and Lidman 2001; Vijayan et al. 1990; Wang et al. 2002). Many animal models of low back pain have documented the role of glial activation in pain and demonstrate increased glial activation in spinal cord tissue for painful injury (Gilmore and Sims 1997; Rutkowski et al. 2002; Sweitzer et al. 2002; Watkins et al. 1995; Winkelstein et al. 2001a). When activated, spinal glial cells upregulate and secrete a variety of pain mediators, including nitric oxide, glutamate, prostaglandins, pro-inflammatory cytokines, and chemokines, which can directly influence neuronal activity (Cavanaugh 2000; DeLeo and Yezierski 2001; Watkins et al. 2001). Also, activation of glial cells can enhance the release of substance P and further regulate neurotransmitter uptake in the spinal cord, having a direct and potent modulating effect on pain (Watkins et al. 2001). While there is an extensive body of work investigating the role of glial activation and neuroimmune changes in chronic low back pain and painful neural injuries, efforts to define such mechanisms for cervical facet injuries and neck pain currently remain undefined.

Rodent Models

Animal models of spinal pain describe a host of electrophysiological, chemical, structural, and behavioral changes associated with nociception and pain (Bennett and Xie 1988; Colburn et al. 1999; Hashizume et al. 2000; Kim and Chung 1992; Obata et al. 2003; Olmarker et al. 2002; Sweitzer et al. 2002; Wang et al. 2002; Winkelstein et al. 2001a,b; Winkelstein and DeLeo 2002; Zhang et al. 1999). In these models, mechanical insults to neural structures, commonly compressive, produce behavioral sensitivity responses mimicking persistent pain symptoms that are also observed clinically (Bennett and Xie 1988; Colburn et al. 1999; Hashizume et al. 2000; Kim and Chung 1992; Obata et al. 2003; Sheather-Reid and Cohen 1998; Winkelstein et al. 2001a,b; Zhang et al. 1999). In low back pain models, behavioral hypersensitivity is commonly measured by mechanical allodynia (pain due to a normally non-noxious stimulus) and is assessed in the dermatome of the injured neural tissue (Colburn et al. 1999; Hashizume et al. 2000). Allodynia is measured by the frequency of paw withdrawals elicited by stimulation with otherwise non-noxious von Frey filaments (Hashizume et al. 2000); it is a useful behavioral outcome as it is also representative of clinical symptoms observed in chronic pain patients, is quantitative, and provides a gauge of nociceptive responses (Barlas et al. 2000; Ochoa 2003; Sheather-Reid and Cohen 1998; Sterling et al. 2003).

The *in vivo* environment afforded by a rodent model of injury offers particular utility for linking mechanics, nociception and behavioral outcomes. In the rat, the dorsal rami of the C6 and C7 nerve roots innervate the C6/C7 facet joint and its capsule. The same spinal nerves extend through the shoulder and arm and into the forepaw (Takahashi and Nakajima 1996), allowing measurement of forepaw allodynia as an indicator and gauge of behavioral sensitivity for C6/C7 facet joint injury. Like the human spine, the quadruped cervical spine is primarily loaded along its long axis, which allows the use of a rodent model in cervical spine biomechanical research (Smit 2002).

Therefore, the primary goal of this study is to examine cervical facet joint mechanics for initiating and modulating pain responses. To this end, a repeatable *in vivo* rodent model of controlled mechanically-induced facet joint distraction has been developed. It is presented here and is used to examine the role of facet joint distraction in pain symptoms. Within the context of this facet joint distraction model, vertebral distractions and capsular strains are quantified during loading, and signs of behavioral pain symptoms are evaluated in the context of C6/C7 facet distraction. Anatomic characterization of the rat facet joint capsule has been performed to address scaling issues and allow comparison with previous human studies in the literature. In addition, one aspect of the CNS nociceptive cascade, glial activation, is examined together with joint distraction and behavioral sensitivity, for insight into the physiologic mechanism of neck pain.

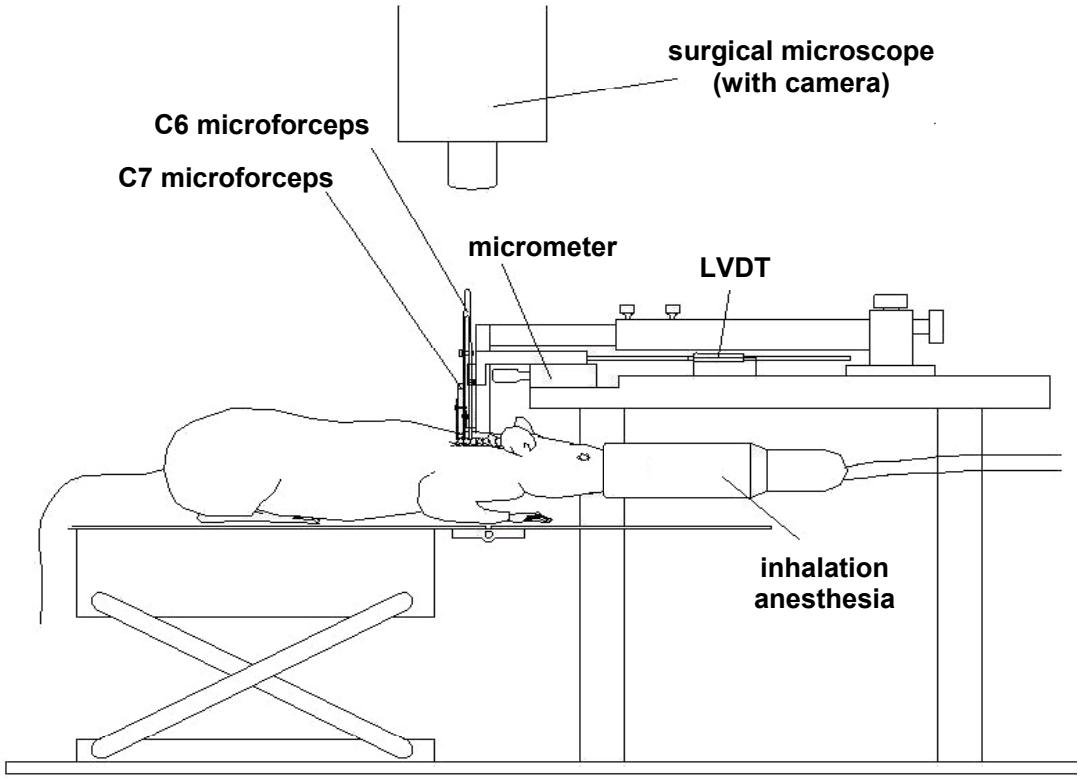

Figure 1. Schematic showing surgical setup and device, with microforceps, manual micrometer, and LVDT. A surgical microscope is mounted above the distraction device for image acquisition. For joint distraction, the C7 microforceps are held rigidly in place while the C6 microforceps are translated rostrally, using the micrometer to impose distraction in the superior direction across the C6/C7 facet joint and its capsular ligament.

METHODS

All experimental procedures have been approved by the University of Pennsylvania Institutional Animal Care and Use Committee (IACUC) and carried out according to the guidelines of the Committee for Research and Ethical Issues of the International Association for the Study of Pain (Zimmermann 1983). Rats were housed under USDA and AAALAC-approved conditions with free access to food and water.

Facet Joint Distraction, Nociception & Pain Symptoms

Surgical Procedure. In order to assess the effect of facet joint injury on pain symptoms, a study was performed to quantify behavioral hypersensitivities after controlled facet joint distraction. Male Holtzman rats, weighing 250-375g, were used in this study. All procedures were performed under inhalation anesthesia (4% halothane for induction, 2.5% for maintenance). Rats were placed in a prone position and the paraspinal musculature separated from the spinous processes from C4-T2. The laminae, facet joints, and spinous processes at C6/C7 were exposed bilaterally under a surgical microscope (Carl Zeiss Inc., Thornwood, NY). Specifically, the supraspinous ligament, interspinous ligament, and ligamentum flavum were resected at C6/C7 to facilitate attachment of the customized device for C6/C7 facet joint distraction (Figure 1). The facet distraction device was rigidly attached to both C6 and C7 spinous processes via microforceps (Figure 2). The C7 spinous process was held fixed and the C6 spinous process translated in the rostral direction. A manual micrometer (Newport Corp., Irvine, CA; 1μm sensitivity) was rigidly coupled to the C6 microforceps and interfaced with a linear variable differential transducer (MicroStrain Inc., Burlington, VT; 8mm stroke, 0.160μm resolution) recording displacements at 10 Hz. Tensile distraction and return of the C6 vertebra was applied manually at a rate of 0.08 mm/s using the micrometer, imposing distraction of the C6/C7 facet joint and its capsule.

Facet Joint Distraction & Vertebral Image Analysis. Facet joint distraction was imposed according to one of the following procedures: (1) subcatastrophic vertebral distraction (*SV*) (target 0.9 mm) (n=6), (2) physiologic vertebral distraction (*PV*) (target 0.1mm)

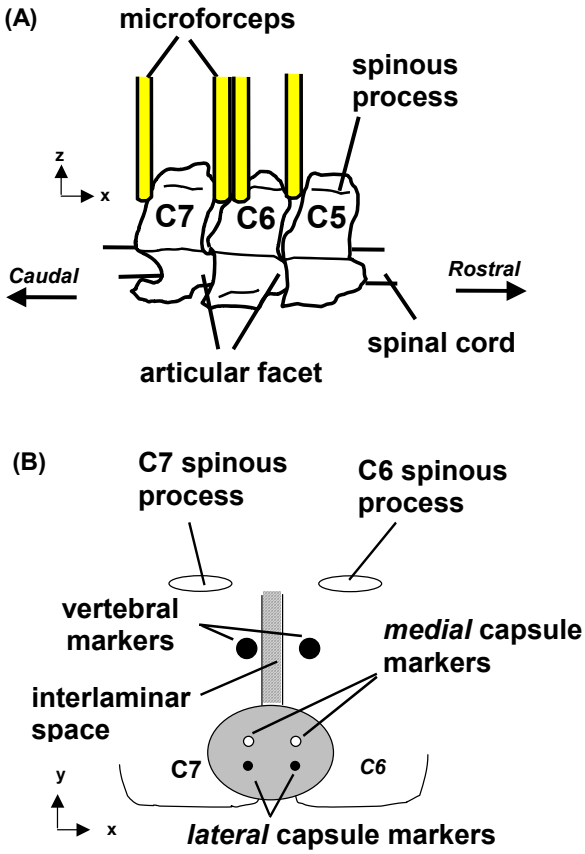

Figure 2. Schematic illustrating the *lateral* view of the placement and attachment of forceps to the C6 and C7 spinous processes (A). For orientation purposes, the plane of the page is the midsagittal plane. Two sets of markers are placed on the facet joint, as shown in a *posterior* view in (B). Vertebral markers (large black circles) are placed on the laminae and used for tracking vertebrae in the behavioral and ligament studies. Capsule markers (small circles) are used to define the nodes of a rectangular element on the capsule in the ligament strain study only. The two small, unshaded (○) circles represent the *medial* pair of capsule markers, while the two small, filled (●) circles represent the *lateral* pair of capsule markers. For reference, x-, y-, and z- directions are shown in both schematics.

(n=6), or (3) *sham* (no distraction) (n=6). For the behavioral study, acrylic black paint markings (diameter=0.36±0.20 mm) were applied to the right C6 and C7 laminae for motion tracking of vertebrae (Figure 2). Capsule markers could not be used in the behavioral study, as methods for their safe and nondestructive removal had not yet been developed or implemented. Marker removal is necessary to minimize confounding effects in postoperative behavioral assessment. During joint distraction, the C6 vertebra was translated to the target distraction (*SV, PV,* or *sham*) and held for 30s, after which time that vertebra was returned to its initial position, unloading the facet joint. The right facet joint and capsule were imaged during distraction at 33 frames/sec using a digital video camera (QImaging, Burnaby, B.C. Canada; 800 x 480 pixels) that was attached to the surgical microscope. Data were acquired using LabVIEW software (National Instruments, Corp., Austin, TX) and displacement and imaging data were synchronized. *Sham* surgeries consisted of device attachment only, for the same duration as the distraction groups. Following surgery, wounds were closed with silk suture and surgical staples. Rats were allowed to recover in room air and were monitored during recovery.

Imposed *in vivo* vertebral distractions were determined using the C6 and C7 vertebral markers (Figure 2). Using Image Pro-Plus software (Media Cybernetics, Inc., Silver Spring, MD), the centroid of

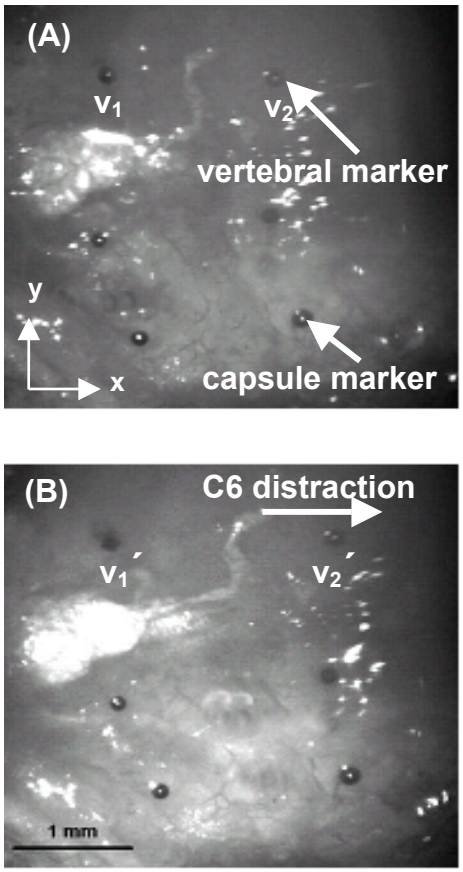

Figure 3. *In vivo* images of the facet joint and capsule for Rat #31: initial condition (A) and maximum distraction condition (B). Also shown are the vertebral and capsule markers. Capsule markers are not used in the behavioral study. For this case, applied vertebral distraction is 0.59 mm. Anatomic orientation is given for reference.

each marker was calculated prior to distraction (initial condition) and at maximal distraction, for each case (Figure 3). All images for each rat were spatially registered to the initial image for that sequence, to account for any system translation during distraction. Vertebral marker positions were defined by their centroids; the horizontal (x-axis) and vertical (y-axis) components of distraction were obtained by subtracting centroid coordinates in the maximum distraction condition from those in the initial condition.

Distraction was applied in the x-direction (Figures 2 & 3), with minimal marker movement in the y-direction relative to movement in the x-direction. As such, vertebral distraction was taken to be distraction in the x-direction only. Vertebral distractions were compared for the distraction groups using a Student's t-test. All statistical analyses for studies were performed using SYSTAT (SYSTAT Software Inc., Richmond, CA) and significance was defined as $p<0.05$.

Behavioral Testing. Following injury, rats were evaluated for bilateral forepaw mechanical allodynia on postoperative days 1, 3, 5, 7, 10, and 14. For each rat, allodynia was measured in both forepaws as the number of withdrawals elicited by a defined non-noxious mechanical stimulus. Prior to injury, rats were acclimated to the testing environment and tester and baseline measurements were recorded for reference. For this study, baseline measurements were negligible, indicating that the stimulus was indeed non-noxious. The same tester, who was blinded to the surgical procedures, performed all behavioral testing for this study. Methods used in this study to measure allodynia have been adapted from well-established methods used for hind paw sensitivity in rodent low back pain models (Decosterd et al. 2002; Kim and Chung 1992; Lee et al. 2004; Rutkowski et al. 2002; Sweitzer et al. 2002; Winkelstein et al. 2001a). They have also been used to detect allodynia changes in a painful cervical nerve root compression model (Hubbard et al. 2003, 2004; Winkelstein et al. 2003). Briefly, in each testing session, rats were subjected to three rounds of 10 tactile stimulations to the plantar surface of each forepaw using 1.4 and 2.0g von Frey filaments (Stoelting Co., Wood Dale, IL). Each of the three rounds was separated by 10 minutes. A positive allodynia response was counted when the rat emphatically lifted its paw upon stimulation, which was accompanied by licking or tightening of the paw. Allodynia responses, as measured by the total number of paw withdrawals for each filament (out of 30 stimulations for each paw, each filament), were compared between forepaws using a paired t-test to test for asymmetry in behavioral sensitivity following injury. To compare the effects of vertebral distraction magnitude on mechanical allodynia across all groups (*SV*, *PV*, or *sham*), a one-way ANOVA with post-hoc Bonferroni correction was used.

Immunohistochemical Staining. Glial activation in the cervical spinal cord was evaluated for markers of activated astrocytes (GFAP) and microglia (OX-42) at day 14 after injury. Animals were deeply anesthetized followed by transcardiac perfusion with 250 ml of phosphate buffered saline (PBS) and 300 ml of 4% paraformaldehyde in PBS (pH 7.4). Following perfusion, spinal cord tissue was exposed by laminectomy, harvested at the C5-C8 levels, and post-fixed in 4% paraformaldehyde for 20 minutes. Samples were transferred to 30% sucrose in PBS and stored for 5 days at 4º C. Tissue was freeze-mounted on cork with Histo Prep (Fisher Diagnostic, Fair Lawn, NJ) for cryostat sectioning. Serial axial C6 spinal cord sections (20μm) from each rat were prepared for free-floating immunohistochemical staining of glial (astrocytes and microglia) activation. A polyclonal antibody to glial fibrillary acidic protein (GFAP) (Dako, Carpinteria, CA), a marker of activated astrocytes, was used at a dilution of 1:20,000. A monoclonal antibody (OX-42) to CR3/CD11b (BD Pharmingen, San Diego, CA) was used as a marker of activated microglia at a dilution of 1:500. Optimal antibody dilutions were determined in pilot studies prior to this investigation. The avidin-biotin technique (Vector Labs, Burlingame, CA) was used to localize areas of activation in each spinal cord section. Negative controls with no primary antibody, as well as naïve tissue sections from normal rats, were included in analysis for normalization and comparison between groups.

Densitometric image analysis techniques were used to quantify glial activation in each sample. The dorsal horn of a representative C6 spinal cord section from each rat was imaged at 50X magnification using a digital camera and stereomicroscope system. Using Image Pro Plus, images were converted to 16-bit grayscale and background-flattened to remove artifacts from any uneven illumination. To assess activation throughout the spinal cord, intensity measurements were taken in several regions, including lamina I, lamina X, and white matter. For normalization purposes, background measurements were also obtained for each cord section. Within each cord region (lamina I, lamina X, white matter, background), 2-3 regions of interest (ROIs) (100 x 100 pixels, corresponding to an area of $0.74mm^2$),

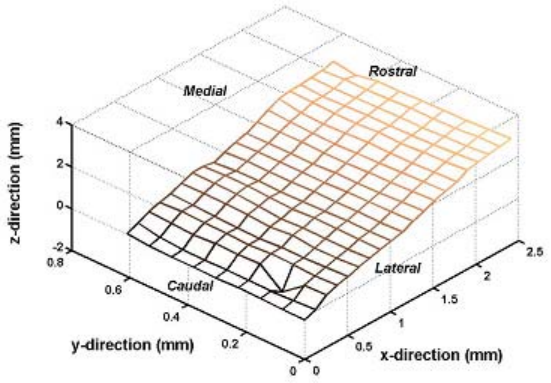

Figure 4. Topographical reconstruction of the facet capsule surface. The capsule has a consistent but apparent slope in z in each of the x- and y-directions. Along the x-direction, the rostral edge is elevated at an inclination angle of 52.2±2.6º with respect to the caudal edge. In the y-direction, the lateral edge is inclined by 7.0±15.0º relative to the medial edge.

were randomly sampled for mean glial staining intensity. The average intensity of all ROIs within that region was calculated, as well as the average intensity of all ROIs in the background. For each rat, the average intensity for each spinal cord region was normalized by its background value. A one-way ANOVA with post-hoc Bonferroni correction was performed to compare mean intensities between injury groups for each spinal cord region. For each injury group, a paired t-test compared the mean intensity differences between lamina I and lamina X to examine regional differences in glial cell activation after joint distraction.

Facet Capsule Topography

To quantify how much the facet capsule forms a planar surface, a customized laser detection device was developed to quantify and reconstruct the surface topography of the rat C6/C7 facet capsule *in situ*. These efforts were also used to examine and validate 2D point reconstruction for strain estimates (see later section). A triangulation laser (1μm resolution, 25μm spot size) (MTI Instruments, Albany, NY) was mounted on a platform above the exposed C6/C7 facet capsule, with a 50mm stand-off distance. The laser interfaced with a dual-axis positioning slide and micrometer (McMaster Carr, Chicago, IL) and a rack and pinion allowed for vertical modification of laser height. Freshly euthanized male Holtzman rats (n=2, 400-500g) were placed in a prone position and paraspinal musculature completely cleared from all cervical spinal levels. As described in the previous section, the right C6/C7 facet joint and its capsule were exposed; care was taken to ensure the capsule was kept moist with saline throughout the measurement session. A capsule surface area of 2.4 mm (rostral-caudal; along x-axis) x 0.6 mm (medial-lateral; along y-axis) was measured for each capsule using the laser (Figure 4). Capsule height data were collected in caudal-to-rostral sequences along the capsule surface (x-direction, Figure 4). Briefly, the capsule height (position in z) was obtained at the lateral corner of the caudal edge of the capsule and incremental values were acquired every 127μm until the laser reached the rostral edge of the capsule. The laser was then returned to the caudal end, incremented in the y-direction by 76μm towards the medial edge of the capsule, and incremental height values were again acquired along the x-direction. This procedure was repeated until a grid of height values was obtained for the entire capsule. For each capsule, a total of 18 sequences in the x-direction and 7 sequences in the y-direction were obtained. For each point, the height value was recorded and imported into MATLAB (The MathWorks Inc., Natick, MA) for visualization and subsequent analysis. Previous validation studies with this technique have quantified an error in measuring height and curvature of 0.93%. The average slope describing height in both x- and y-directions was calculated and compared across each incremental sequence in each direction to quantify the relative orientation of the capsule's plane relative to the plane of imaging.

***In Vivo* Facet Capsule Ligament Strains**

Surgical Procedure & Facet Distraction. To further investigate the hypothesis that facet-mediated pain may be initiated by facet capsule ligament mechanical behavior, a characterization of local ligament strain during distraction injury was performed using male Holtzman rats (weighing 400-500 g). Preliminary studies have indicated that allodynia responses are not significantly different (p=0.38) for rats of different weight ranges in this injury model. As such, while it is recognized that the rats used in this study are heavier than those used in the behavioral study, effects are taken as minimal. Surgical preparation, vertebral distraction techniques, and imaging procedures were identical to those described in the earlier section for the behavioral study. In this ligament study, polystyrene magnetic particles (diameter = 0.17±0.01 mm) (Spherotech, Inc., Libertyville, IL) were used for motion tracking. Two particles were placed on the C6 and C7 laminae as before, to serve as the vertebral markers. In addition, two particles were placed on each of the rostral and caudal regions of the C6/C7 capsule,

(Figure 3), creating a grid of four points for capsular strain calculations. Facet joint distraction was imposed according to one of the same vertebral distractions as in the behavioral study: (1) subcatastrophic vertebral distraction (*SV*) (n=5) or (2) physiologic vertebral distraction (*PV*) (n=5). For each group, distractions were calculated and compared using a Student's t-test.

Capsule Strain With Marker Projection. Capsule particle positions were digitized for both initial and maximum distraction conditions. Because a single camera was used to measure marker positions, geometric analyses were performed to mathematically accommodate the capsule's geometry relative to image data for strain calculations. Topographic reconstruction of the facet capsule surface showed a consistent but apparent slope across the capsule in both x- and y-directions (Figure 4). There was a positive slope in the x-direction, with the rostral edge of the facet capsule inclined by 52.2±2.6º with respect to the caudal edge. Also, the lateral capsule edge was inclined by 7.0±15.0º relative to the medial edge, resulting in a positive slope in the y-direction. Despite the capsule's inclination out of the plane parallel to the image plane, the rostral and caudal capsule markers are placed artificially in the same plane due to planar imaging. Because the C6 vertebra is distracted rostrally relative to the C7 vertebra, the 52.2±2.6º inclination measured in the positive x-direction contributes to underestimations in calculated strain compared to those actually produced in the capsule. In contrast, for a given capsule length, the 7° inclination in the y-direction would artificially alter the length in this direction by only 1%. Because this effect is small with regard to calculated strains, it was determined that error contribution from the inclination in the y-direction was minimal.

To account for the effects of the 2D imaging system in capsule strain calculations, the x-coordinates of the C7 capsule markers, which lie out of the plane parallel to the image plane, were projected into the imaging plane (Figure A1, see Appendix for calculations). For both medial and lateral pairs of capsule markers (Figure 2), the x-coordinate of the rostral centroid (C6) was set as reference (x=0) and the x-coordinate of the caudal centroid (C7) was mathematically adjusted to account for inclination out of plane. This projection factor accounts for the 52.2º inclination of the capsule along the positive x-axis and allows for the x-coordinates of the rostral and caudal markers to be accurately represented in the same plane.

Using the original C6 coordinates and projected C7 coordinates, the capsule marker centroids formed the nodes of a single four-sided finite element. Strains were calculated in MATLAB using specialized code, adapting the 2D isoparametric finite element method of Hoffman and Grigg (1984) (Ianuzzi et al. 2004). For each element, horizontal (*u(x,y)*) and vertical (*v(x,y)*) nodal displacements for maximal distraction were used to calculate Lagrangian strain (*E*) values:

$$E_{xx} = \frac{\partial u}{\partial x} + \frac{1}{2}\left[\left(\frac{\partial u}{\partial x}\right)^2 + \left(\frac{\partial v}{\partial x}\right)^2\right]$$

$$E_{yy} = \frac{\partial v}{\partial y} + \frac{1}{2}\left[\left(\frac{\partial v}{\partial y}\right)^2 + \left(\frac{\partial u}{\partial y}\right)^2\right] \quad (1)$$

$$E_{xy} = \frac{1}{2}\left[\frac{\partial u}{\partial y} + \frac{\partial v}{\partial x} + \left(\frac{\partial u}{\partial x}\right)\left(\frac{\partial u}{\partial y}\right) + \left(\frac{\partial v}{\partial x}\right)\left(\frac{\partial v}{\partial y}\right)\right]$$

In Eqn. (1), both *u* and *v* are functions of *x* and *y* positions. The strain tensor [*E*] was then transformed into [*E'*] using a rotation matrix ([T]) (Lai et al. 1993), to accomodate any physiological rotation that occurred during joint distraction:

$$E' = [T]E \quad (2)$$

Principal capsule strains and directions were also calculated by solving for the eigenvalues and eigenvectors of [*E'*]. Methods were validated by strain calculations for several known combinations of internodal displacement and rotation. For *SV* and *PV*, a comparison of mean maximum capsule principal strain and direction was performed using a Student's t-test.

RESULTS

During all loading, no gross ligamentous injury was observed. In addition, at the study's completion (day 14), examination of the facet capsule under the surgical microscope indicated no gross mechanical injury to the capsule in any of the rats. After surgery, all rats demonstrated normal functioning with grooming and consistent weight gain. They had normal head mobility, indicating no adverse effects of the surgical and loading procedures on neck mobility.

Gross mechanical and allodynia data from a subset of rats in each of the *SV* and *PV* groups have been published as part of a larger characterization study of this model (Lee et al. 2004). For animals used in the

Table 1. Imposed facet joint distraction injury metrics for each rat in the behavioral study and averages for *SV* and *PV* groups. Forceps displacement was used as guidance for input of controlled injury conditions. Total allodynia is the sum of all paw withdrawal responses over the 14-day postoperative period (on each of days 1,3,4,7,10,14) and is used as a measure of cumulative hypersensitivity for each rat. Behavioral data from a subset of these rats in each of the *SV* and *PV* groups has been published previously (Lee et al. 2004).

Rat ID	Forceps Displacement (x) (mm)	Vertebral Distraction (x) (mm)	Vertebral Distraction (y) (mm)	Distraction Rate (mm/s)	Total Allodynia (average of both forepaws; 2.0g)
K4	1.22	0.21	-0.05	0.07	28
5	1.65	0.72	0.05	0.09	29.5
8	1.51	0.53	-0.01	0.09	32.5
17	1.36	1.53	0.12	0.07	43
18	1.33	1.51	-0.09	0.06	45
20	1.19	0.89	-0.42	0.06	45.5
SV Avg (SD)	***1.38 (0.18)***	***0.90 (0.53)***	***-0.07 (0.19)***	***0.07 (0.01)***	***37.25 (8.12)***
K1	0.51	0.14	0.02	0.08	13
K7	0.52	0.23	-0.02	0.11	9.5
K11	0.51	0.17	0.01	0.10	10
6	0.81	0.28	-0.01	0.14	16.5
11	0.63	0.12	-0.02	0.06	8.5
21	0.44	0.20	0.11	0.05	10
PV Avg (SD)	***0.57 (0.13)***	***0.19 (0.06)***	***0.01 (0.05)***	***0.09 (0.03)***	***11.25 (2.98)***

behavioral study, mean applied vertebral distraction was 0.90±0.53 mm and 0.19±0.06 mm in the *SV* and *PV* groups, respectively (Table 1). There was a significant difference in applied vertebral distraction between *SV* & *PV* (p=0.004) (Table 1). Digitization errors were 0.006±0.003 mm, only 0.006% and 0.03% of the imposed displacements in *SV* and *PV*, respectively, for these studies. These errors were small compared to applied vertebral distractions, suggesting that these errors did not contribute substantially to calculated distraction values. No significant difference was found between the applied distraction rate (0.08±0.03 mm/s) for *SV* & *PV* (Table 1). Vertebral distractions in the y-direction were small (7.8% and 5.3% of applied distraction in the x-direction for *SV* and *PV*, respectively). *Sham* distractions were low (0.003±0.001 mm) and within the digitization error range.

Mechanical allodynia was not significantly different between the left and right forepaws for either distraction injury or *sham* (both filament strengths, $p>0.19$). As such, left and right allodynia responses for each rat were averaged for all between-group analyses. For *SV* distraction injuries, allodynia was immediately increased over baseline on day 1 (Figure 5) and demonstrated a slight decrease over time, indicating prolonged and maintained behavioral hypersensitivity. Allodynia for *PV* distraction was not significantly different from *sham* levels at any time point for either von Frey filament (Figure 5).

Allodynia for *SV* distraction was significantly elevated over both *PV* distraction ($p<0.008$, 1.4g; $p<0.004$, 2g) and *sham* ($p<0.003$, 1.4g; $p<0.001$, 2g) for the entire postoperative period, with the exception of testing with the 1.4g filament on postoperative day 14 (Figure 5). *Sham* responses were low and not different from baseline values at any time point. In addition, total mechanical allodynia over the entire postoperative period was calculated for each rat in the *SV* and *PV* distraction groups as a measure of cumulative hypersensitivity. Total allodynia in the *SV* group (37.25±8.12 withdrawals) exhibited a three-fold increase in sensitivity compared to the *PV* group (11.25±2.98 withdrawals), for a nearly five-fold

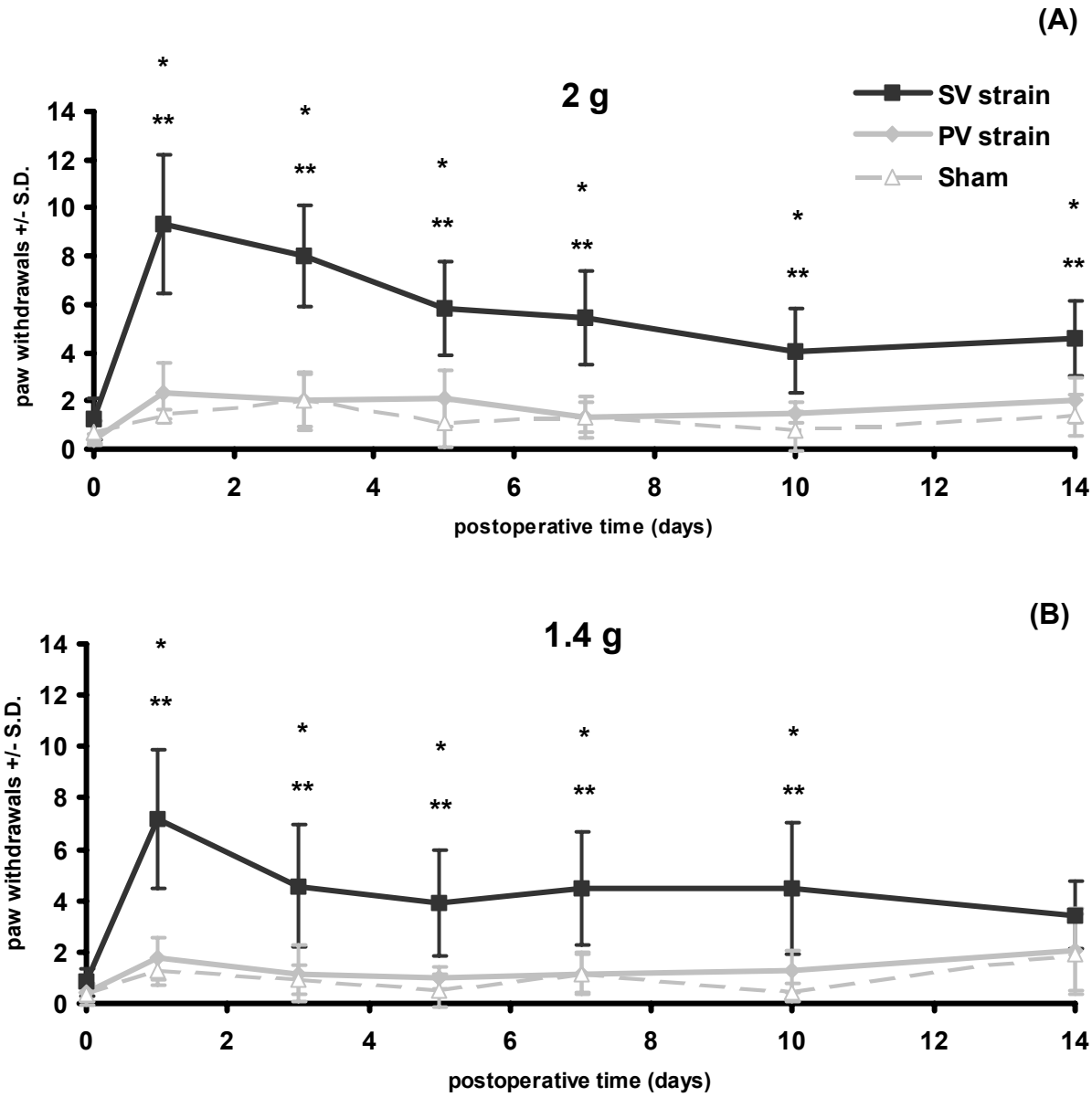

Figure 5. Average forepaw mechanical allodynia as measured by the number of paw withdrawals for *SV* distraction, *PV* distraction, and *sham*. Higher numbers of paw withdrawals correspond to increased sensitivity. *SV* distraction produced significantly increased allodynia over *PV* (*) and *sham* (**) that was maintained over the 14-day testing period, for testing with the 2g von Frey filament (A). Results were confirmed for testing with the 1.4g filament, with the exception of day 14 (B).

difference in vertebral distraction for these two groups (Table 1).

Astrocytic activation was evident in all rats, with varying degrees of intensity for cord region and injury type (Figures 6 & 7, Table A1). Tissue from one rat (#K1) in the *PV* group was not available for analysis because its integrity was not maintained during the staining process. GFAP staining in white matter did not vary between *SV*, *PV*, or *sham*. In fact, these intensities were quite consistent among rats, as would be expected for this region of the cord. However, in general, dorsal horn GFAP reactivity was elevated for *SV* over *PV* and *sham*, while *PV* and *sham* were not different from each other. Specifically, astrocytic activation for *SV* in lamina I

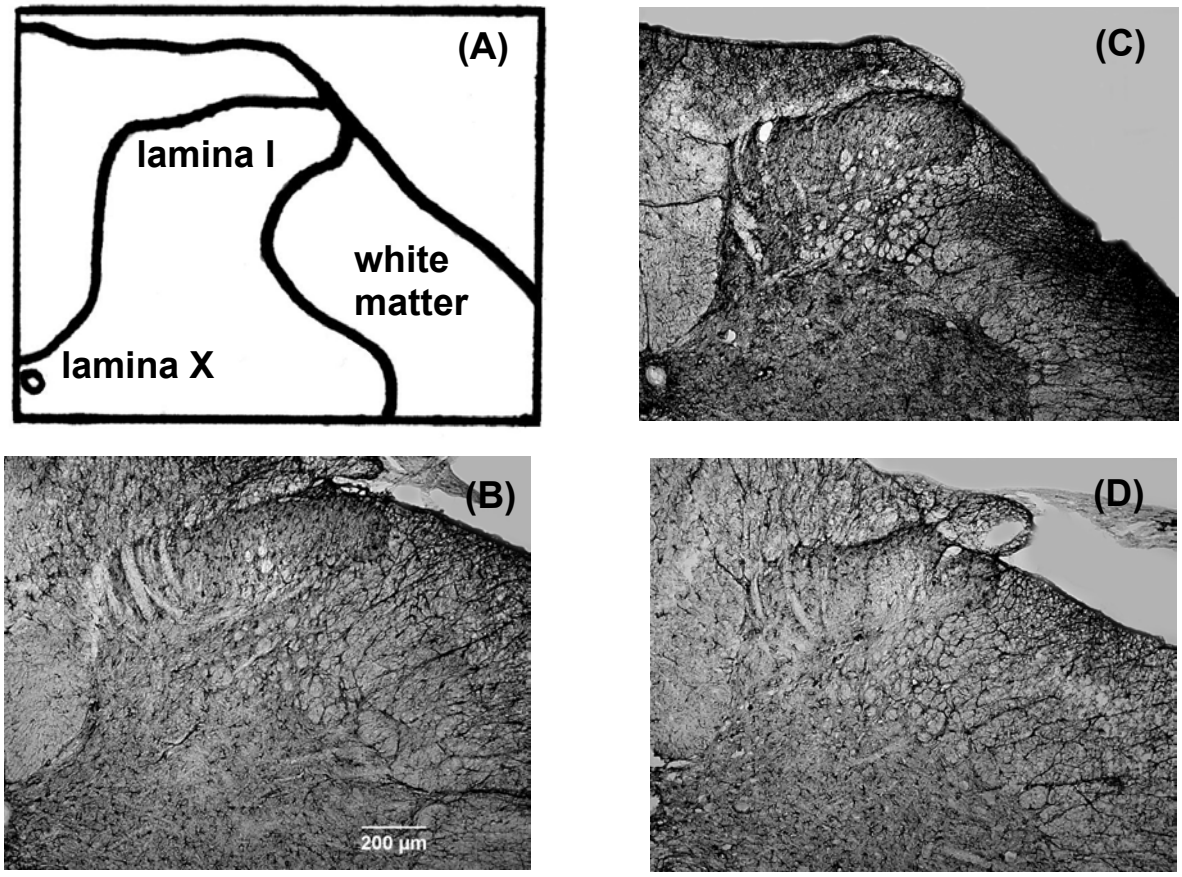

Figure 6. Representative images depicting astrocytic activation in the dorsal horn region of the cervical spinal cord at post-injury day 14. Mean activation intensity was quantified for each section at locations in the dorsal horn (lamina I, lamina X) and white matter (A). Shown are images from *SV* distraction (C) (Rat #20), *PV* distraction (D) (Rat #21), and *sham* (B) (Rat #22) cases. Activation in the spinal cord for *SV* injury is generally greater than *PV* and *sham* injuries. These data are specifically quantified in Figure 7.

was more intense than both *PV* and *sham* (Figures 6 & 7, Table A1). While trends indicate greater astrocytic activity in lamina I for *SV* above *PV* and *sham*, *SV* was only significantly different from *sham* ($p=0.049$). *PV* GFAP reactivity was only slightly increased over sham in lamina I. Astrocytic activation for *SV* injury also was elevated over *PV* and *sham* in both lamina X and white matter. GFAP reactivity for *PV* injury was not significantly different from sham for these other spinal regions (lamina X and white matter). Comparing regions of the dorsal horn, astrocytic activation was the most intense in lamina X for each injury group (Figure 7, Table A1). Unlike the graded astrocytic response observed with GFAP staining, microglial activation intensity was not significantly different between any group in any of the spinal cord regions (Figure 7), although *SV* showed trends of greatest reactivity. A comparison of OX-42 reactivity across regions revealed no significant difference in microglial activation between spinal cord regions for each injury group. Interestingly, while a nearly five-fold increase in vertebral distraction produced a three-fold increase in resultant mechanical allodynia, a similar relationship was not produced for either astrocytic or microglial activity for any group.

For the capsular ligament study, mean applied vertebral distractions in *SV* and *PV* groups were 0.57±0.11 mm and 0.20±0.05, respectively; as in the behavioral study, these two groups were significantly different ($p<0.0005$). For applied distraction, mean maximum principal capsule strain was 27.7±11.9% and 8.1±2.4% for *SV* and *PV*, respectively (Table 2). Also, for the ligament study, neither the applied rate (0.10±0.02 mm/s) nor magnitudes (*SV* & *PV*) of applied vertebral distraction was significantly different from those applied in the behavioral study. The principal capsule strains for *SV* and *PV* injury were significantly different from each other ($p<0.0005$). Principal directions associated with the maximum principal capsule strains were generally oriented across the joint, along the direction of loading, and were only 9.7±4.4° and 10.9±3.5° off the x-axis for *SV* and *PV*, respectively (Table 2). For an approximate three-fold increase in applied

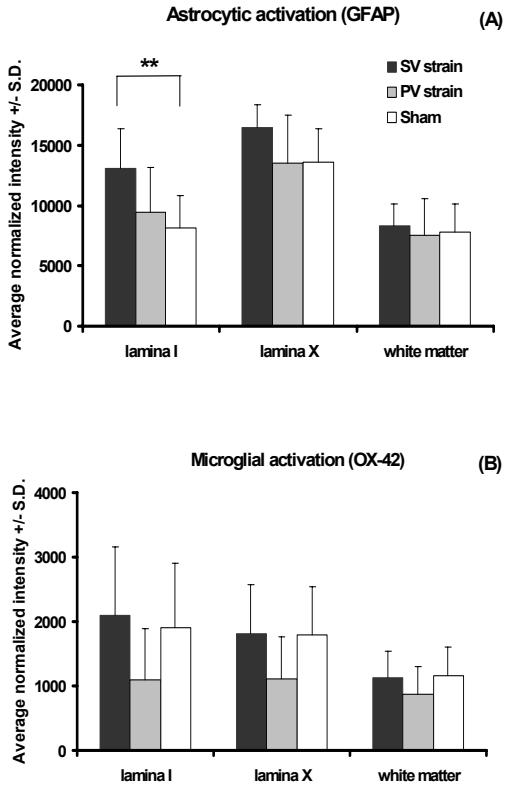

Figure 7. Average normalized staining intensity for astrocytic (A) and microglial (B) activation by group at post-injury day 14. Average staining intensity is presented by spinal cord region (lamina I, lamina X, white matter) for each injury (*SV*, *PV*, *sham*). Significant differences were found only between *SV* and *sham* (**) in lamina I for GFAP staining. Overall OX-42 staining (microglia) was unchanged for the different injury groups.

vertebral distraction, a resultant three-fold increase in mean maximum principal capsule strain is observed, indicating that for the anatomic placement of the markers used in this study, there is a direct linear relationship between vertebral distraction and capsule strain.

Recognizing that the behavioral and ligament studies separately report pain symptom and mechanical data for ligament tension, preliminary studies (n=4; data not shown) used smaller rats (331±11 g) to investigate capsule strain data in the context of pain-producing joint distractions. In these studies, rats of comparable weights to those in the behavioral study underwent vertebral distractions of 0.9 mm, matching mean distractions in Table 1, and sufficient for producing sustained allodynia. For these vertebral distractions, mean maximum principal strain in the capsule was 34.3±24.6%. Also, these mean maximum principal strains were not significantly different (p=0.65) from those produced for the *SV* group in the ligament study (using larger sized rats; Table 2). These limited data help provide mutual context between the findings of the two studies reported here (Tables 1 & 2; Figure 5).

DISCUSSION

This study demonstrates a direct relationship between mechanical facet joint distraction and resultant behavioral sensitivity and one indicator of spinal sensitivity, glial activation. The results demonstrate that vertebral distractions of 0.90±0.53 mm (*SV*) across the C6/C7 facet joint in the rat are sufficient to induce and maintain mechanical allodynia in the forepaw (Figure 5). For applied vertebral distractions of lower magnitude (0.19±0.06 mm=*PV*), behavioral sensitivity was not produced at levels significantly different from *sham* or baseline. These findings directly relate mechanical facet loading and pain symptoms and further suggest that a distraction threshold exists for facet distraction above which persistent pain symptoms can be produced and maintained.

The distraction device presented here provides utility for applying controlled and repeatable facet joint distraction, allowing for control of mechanical injury parameters including distraction magnitude, distraction rate, and hold duration. This study aimed to apply tension across the facet joint along the long-axis of the cervical spine to impose the most direct and severe insult to the capsule. Distraction components in the y-direction were small compared to the primary motions of applied distraction in the x-direction, confirming symmetric joint distraction along the spinal axis (Figure 3, Table 1). Additional support for distraction symmetry is confirmed by the lack of difference in allodynia responses between the right and left paws. Also, *sham* distractions were within the digitization error range and support these *sham* procedures as an appropriate control. While it is recognized that many different injury mechanisms of facet-mediated whiplash neck pain have been hypothesized in the literature (Kaneoka et al. 1999; Ono et al. 1997; Panjabi et al. 1998a,b; Pearson et al. 2004; Yoganandan et al. 1998, 2001, 2002), this study has addressed only one such loading paradigm—capsular ligament tension. This is based on previous evidence of subcatastrophic ligament failure in tension (Winkelstein et al. 2000) and provides a direct measure of injury and means for activating nociceptors by capsule stretch. The study presented here applied distraction at a quasistatic rate (0.08 mm/s). While the whiplash event occurs over a

Table 2. Average vertebral distraction and principal capsular strain and direction for individual rats in ligament strain study.

Rat ID	Vertebral Distraction (x) (mm)	Vertebral Distraction (y) (mm)	Principal Capsule Strain (%)	Principal Capsule Strain Direction (Oriented Relative to x-axis) (°)*
27	0.61	-0.19	35.2	-7.21
28	0.58	-0.11	41.9	8.09
29	0.38	-0.06	10.6	17.44
31	0.59	-0.12	25.1	-7.72
32	0.69	-0.17	25.8	7.77
SV Avg (SD)	***0.57 (0.11)***	***-0.13 (0.05)***	***27.7 (11.9)***	***9.65 (4.40)****
27	0.24	-0.06	10.2	-15.43
28	0.20	-0.02	10.3	6.42
29	0.12	-0.02	5.1	13.06
31	0.22	-0.06	9.1	-8.81
32	0.24	-0.15	6.3	10.60
PV Avg (SD)	***0.20 (0.05)***	***-0.06 (0.05)***	***8.1 (2.4)***	***10.87 (3.52)****

* (+) and (-) angles of principal strain orientations are provided. The average of the absolute values of each angle was calculated to obtain group averages.

much more rapid time course, ligament deformation responses with respect to failure, or subcatastrophic failure, have been shown to be independent of loading rate (Pintar et al. 1992; Winkelstein et al. 1999). Further, Khalsa et al. (1996) have demonstrated receptor responses to be driven by displacements, which are not altered by rate of ligament loading. The distraction device and procedure presented here offer a novel method of applying controlled tension across the facet joint and is a useful setup for examining the effects of facet joint distraction in an *in vivo* setting. The findings presented here offer a foundation for future understanding in higher rate studies.

This study's examination of the rat facet capsule curvature documents its being largely oriented in one plane. The facet capsule is inclined along the long axis of the spine (x-axis), with little sloping along the medial-lateral direction (Figure 4). The variability of these slopes across the capsule is small and further supports the capsule surface being estimated as planar. Moreover, it further minimizes the need for 3D point location in this model for this mode of loading, which is often required for human cadaveric studies, as the human capsular ligament has a distinct spherical curvature to it (Pearson et al. 2004; Siegmund et al. 2001; Winkelstein et al. 2000; Yoganandan et al. 2002). This is particularly relevant in a rat model where size is a distinct limitation. The depth of the surgical incision and small size of the rodent facet capsule (2.4 mm x 0.6 mm) prevent the use of multiple cameras in the current model of joint distraction presented here. While limiting the characterization of the 3D positional displacement of the capsule, the use of a single camera is sufficient for capsule marker tracking in this study given the uniform capsule inclination (Figure A1).

This study is the first to directly demonstrate behavioral hypersensitivity after facet joint distraction injury and suggests that a correlative relationship between the two may exist. The significant increase in mechanical allodynia after *SV* distraction compared to *PV* distraction or *sham* injury (Figure 5) suggests that capsule distraction may play a role in initiating or contributing to neck pain after joint distraction injury. Specifically, the three-fold increase in total allodynia for a nearly five-fold increase in vertebral distraction (Table 1) suggests a nonlinear relationship may exist between mechanical

loading of this joint and the nature of the amount of behavioral sensitivity. Allodynia responses for *sham* surgeries were not different from baseline values (Figure 5), despite the fact that *sham* procedures involved the same surgery as the distraction injury, including ligament resection and device attachment, but no joint distraction. However, it should be noted that *PV* distraction did not produce sensitivity different from *sham*. Therefore, further studies are required to investigate the relationship between joint distraction and resultant symptoms and to determine the magnitude of this threshold for injury.

The results of the ligament strain study offer *in vivo* characterization of local facet joint mechanics (vertebral and capsular) during joint distraction in the context of pain. Together with the results of the behavioral study, these findings suggest that a threshold for the generation and maintenance of facet-mediated pain behaviors exists. This capsule ligament study indicates that C6/C7 facet maximum capsule strains ranging between 11 and 42% (Table 2) may be sufficient to generate neck pain after injury. Joint distraction produced in this study was primarily directed across the joint and did not directly incorporate a sagittal bending component for vertebral kinematics. However, maximum capsular strains for pure vertebral bending have been previously reported as 12.1±2.5% and 11.6±2.6% for flexion and extension, respectively (Winkelstein et al. 2000), which are comparable to the *PV* distraction condition in this study. Additional studies demonstrate that whiplash-like combined shear, bending, and compression produce subcatastrophic failure of the capsule at strain values of 35±21% (Siegmund et al. 2001), which is consistent with the range and strains in the *SV* condition examined here. The lack of difference in behavioral hypersensitivity and glial activation after the imposition of *PV* distraction in comparison to *sham* injury suggest that these levels of facet joint distraction may not produce neck pain. Further, previous studies have shown that subcatastrophic ligament injuries can occur during whiplash simulations (Panjabi et al. 1998b; Pearson et al. 2004) and that such injury leaves ligaments grossly intact while microscopic failures may occur during loading (Winkelstein et al. 2000). While this study did not explicitly examine the facet capsule for evidence of *subcatastrophic* damage after distraction injury, efforts (mechanical and/or histological) would provide further characterization and interpretation of the mechanical and physiological meaning of these injuries in the context of neck pain. The data presented here provide a direct link between these injuries and the potential for neck pain. They support the hypothesis that under subcatastrophic loading conditions, like those produced in whiplash injury, pain symptoms may be produced and/or maintained and provide quantitative data linking previously speculative mechanical studies.

Several mechanisms of facet joint injury have been hypothesized to contribute to neck pain after whiplash injury, including facet pinching, sliding, compression, and tension (Kaneoka et al. 1999; Luan et al. 2000; Ono et al. 1997; Panjabi et al. 1998a,b, 2004; Pearson et al. 2004; Yoganandan et al. 1998, 2002). However, analysis of whiplash kinematics has demonstrated significantly increased capsule strain during injury (Panjabi et al. 1998b; Pearson et al. 2004; Siegmund et al. 2001; Winkelstein et al. 2000), implicating joint tension as a potential injury mechanism. In addition, animal models have demonstrated alterations in neural electrical activity following lumbar facet capsule tension, including the activation of mechanoreceptive and nociceptive fibers (Avramov et al. 1992; Cavanaugh et al. 1989, 1996; Khalsa et al. 1996; Pickar and McLain, 1995; Yamashita et al. 1990). These data suggest that stretch-induced activation of capsule fibers may be a mechanism of initiating physiologic responses that manifest in pain symptoms.

While our study examines vertebral distraction and capsular strains across the facet joint in the context of pain symptoms, it is recognized that the mode of loading imposed for facet capsule distraction may simultaneously load other anatomical structures in the spine (e.g. intervertebral disc) due to bending in the sagittal plane. For example, the distraction protocol used in this study imposes flexion across the intervertebral space, which results in both a tensile load across the facet capsule and also potential compression of the intervertebral disc. As such, continued investigations are needed using this injury model to quantify the flexion bending moment and associated compressive load applied to the disc. Because injury to such structures may also contribute to behavioral sensitivity and neck pain, efforts are needed to characterize associated tissue loading in this model and investigate the potential role of injury to other spinal structures in generating behavioral sensitivities in neck pain. However, the results presented here, in conjunction with biomechanical evidence in the literature, provide additional evidence to support the hypothesis that injury to the facet joint has a direct effect on pain symptom generation.

Mechanical allodynia results from a host of nociceptive physiologic changes in the central nervous system, including neuronal plasticity, glial cell activation, and cytokine upregulation (DeLeo and

Yezierski 2001; Hashizume et al. 2000; Ji and Woolf 2001; Rutkowski et al. 2002; Watkins et al. 1995; Winkelstein et al. 2001b). Allodynia has been shown to be directly correlated with and to require these changes in models of low back pain. The current study examined one element of the CNS response, glial cell activation and pain symptoms in the context of facet joint distraction. Several studies using lumbar pain models have demonstrated a temporal correlation of astrocytic activation with allodynia after injury (Colburn et al. 1999; Hashizume et al. 2000; Winkelstein et al. 2002). These same studies show that, unlike astrocytes, the amount of microglial activation does not directly correlate with the degree of behavioral sensitivity. This same dissociation between allodynia and microglial activation is also observed in the present study by the lack of differential activation between any group (Figure 7). However, the increased astrocytic activation for *SV* distraction compared to *PV* distraction and *sham* injury was evident and may provide a physiologic mechanism of allodynia and pain symptoms. This study specifically examined activation in those spinal laminae in the dorsal horn that are involved in relaying sensory information about pain (Kandel et al. 2000). Laminae I and X (Figure 6) have been shown to have the heaviest concentration of spinal SP binding sites (Doyle and Hunt 1999), which suggests that these laminae are particularly important in pain transmission. Moreover, in that study, NK-1 (receptor for substance P) expressing neurons in lamina I were shown to specifically encode information about stimulus intensity, while lamina X was hypothesized to play a role in mediating joint pain (Doyle and Hunt 1999). Therefore, in this study, the specific increase in astrocytic activation in lamina I after *SV* injury suggests that nociceptive changes resulting from subcatastrophic facet capsule strain may lead to a CNS response that triggers glial activation. In contrast, *PV* capsule distraction may not be sufficient to initiate these nociceptive processes, which may explain the lack of *PV* glial activation and elevated allodynia seen in this study. Further, the lack of difference in astrocytic activation across groups within lamina X suggests that injury magnitude may not differentially affect nociception within the deeper laminae for painful ligamentous injury and may be indicative of general joint injury. While astrocytic activation after facet distraction injury offers cellular evidence to support the role of facet-mediated injury in pain, continued efforts are needed to fully understand specific contributions to pain symptoms and mechanical thresholds for their activation. Data presented here (Figures 5 & 7, Table 1) for allodynia and astrocyte reactivity, which show different response characteristics for mechanical insult magnitudes, suggest there may be different mechanical thresholds for behavioral and nociceptive outcomes.

Increasing evidence strongly implicates glial cells in the production and maintenance of persistent pain states (Watkins et al. 2001). Glial cells play an active role in modulating neural communication and once activated, are able to enhance the release of nociceptive neurotransmitters that may act as pain modulators. While glial activation is an important element in nociceptive cascades, there is a host of other biomechanical and cellular responses that are initiated after injury and contribute to pain. Some of these events may involve nociceptive neurotransmitters, like substance P and CGRP, or changes in neural electrical activity. In fact, given the dissociation between allodynia and spinal astrocytic activation for injury magnitude, it is likely possible that glial responses may be only one contributor to behavioral sensitivity following capsule distraction. Other neurochemical responses may dominate, as allodynia expressed a nearly three-fold increase between *PV* and *SV* distractions (Table A1), yet astrocytic activation showed only a 1.5-fold increase. Further investigation into the effect of these and other CNS changes is ultimately necessary for understanding the mechanisms between mechanical injury and the development of persistent neck pain and will be useful in the development of potentially effective therapeutic interventions.

CONCLUSION

Numerous studies have implicated the facet joint in neck pain, however, this study is the first to provide physiological and behavioral support for its involvement in pain generation by demonstrating behavioral hypersensitivities and increased glial activation after imposition of subcatastrophic vertebral distraction. In addition, for these painful injuries, spinal astrocytic activation was also increased in laminae I and X, which may be indicative of a physiologic mechanism of pain. This glial activation is only part of a cascade of molecular and cellular changes that contribute to central sensitization and persistent pain. Indeed, in clinical research, central sensitization has been hypothesized as a mechanism of chronic pain after whiplash injury (Banic et al. 2004; Barlas et al. 2000; Curatolo et al. 2001; Kivioja et al. 2001). Moreover, the mechanical data together with behavioral findings suggests a capsule strain-based threshold for neck pain after joint distraction injury exists between 11-42%. Continued studies simultaneously quantifying facet capsule mechanics and pain behaviors will provide

more insight and clarification in understanding this joint's potential for generating pain. Taken together, the findings presented in this study indicate a relationship between mechanical injury to the facet joint and its ability to produce pain.

ACKNOWLEDGMENTS

This work was funded by grant support from the Whitaker Foundation (RG-02-0311), the Catharine D. Sharpe Foundation, and a graduate fellowship from the National Science Foundation.

REFERENCES

April, C., and Bogduk, N. (1992) The prevalence of cervical zygapophyseal joint pain. Spine 17(7): 744-747.

Avramov, A.I., Cavanaugh, J.M., Ozaktay, C.A., Getchell, T.V., and King, A.I. (1992) The effects of controlled mechanical loading on group-II, III, and IV afferent units from the lumbar facet joint and surrounding tissue. The Journal of Bone and Joint Surgery 74-A(10): 1464-1471.

Banic, B., Petersen-Felix, S., Andersen, O.K., Radanov, B.P., Villiger, P.M., Arendt-Nielsen, L., and Curatolo, M. (2004) Evidence for spinal cord hypersensitivity in chronic pain after whiplash injury and in fibromyalgia. Pain 107: 7-15.

Barlas, P., Walsh, D.M., Baxter, G.D., and Allen, J.M. (2000) Delayed onset muscle soreness: effect of an ischaemic block upon mechanical allodynia in humans. Pain 87: 221-225.

Barnsley, L., Lord, S., and Bogduk, N. (1993) Comparative local anaesthetic blocks in the diagnosis of cervical zygapophysial joint pain. Pain 1993: 99-106.

Barnsley, L., Lord, S., and Bogduk, N. (1994) Whiplash injury. Pain 58: 283-307.

Beamen, D.N., Graziano, G.P., Glover, R.A., Wojtys, E.M., and Chang, V. (1993) Substance P innervation of lumbar spine facet joints. Spine 18(8): 1044-1049.

Bennett, G.J., and Xie, Y.-K. (1988) A peripheral mononeuropathy in rat produces disorders of pain sensation like those seen in man. Pain 33(1): 87-107.

Bogduk, N., and Marsland, A. (1988) The cervical zygapophysial joints as a source of neck pain. Spine 13(6): 610-617.

Cavanaugh, J.M., El-Bohy, A., Hardy, W.N., Getchell, T.V., Getchell, M.L., and King, A.I. (1989) Sensory innervation of soft tissues of the lumbar spine in the rat. Journal of Orthopaedic Research 7: 378-388.

Cavanaugh, J.M., Ozaktay, A.C., Yamashita, H.T., and King, A.I. (1996) Lumbar facet pain: biomechanics, neuroanatomy, and neurophysiology. Journal of Biomechanics 29(9): 1117-1129.

Cavanaugh, J.M. (2000) Neurophysiology and neuroanatomy of neck pain. In Frontiers in Whiplash Trauma: Clinical and Biomechanical, ed. N. Yoganandan and F.A. Pintar, pp. 79-96. IOS Press, Amsterdam.

Colburn, R.W., Rickman, A.J., and DeLeo, J.A. (1999) The effect of site and type of nerve injury on spinal glial activation and neuropathic pain behavior. Experimental Neurology 0: 1-16.

Curatolo, M., Petersen-Felix, S., Arendt-Nielsen, L., Giana, C., Zbinden, A.M., and Radanov, B.P. (2001) Central hypersensitivity in chronic pain after whiplash injury. The Clinical Journal of Pain 17: 306-315.

Cusick, J.F., Pintar, F.A., and Yoganandan, N. (2001) Whiplash syndrome. Spine 26(11): 1252-1258.

Decosterd, I., Allchorne, A., and Woolf, C.J. (2002) Progressive tactile hypersensitivity after a peripheral nerve crush: non-noxious mechanical stimulus-induced neuropathic pain. Pain 100(1-2): 155-162.

DeLeo, J.A., and Yezierski, R.P. (2001) The role of neuroinflammation and neuroimmune activation in persistent pain. Pain 90: 1-6.

Doyle, C.A., and Hunt, S.P. (1998) Substance P receptor (neurokinin-1)-expressing neurons in lamina I of the spinal cord encode for the intensity of noxious stimulation: a c-Fos study in rat. Neuroscience 89(1): 17-28.

El-Bohy, A.A., Goldberg, S.J., and King, A.I. (1987) Measurement of facet capsular stretch. 1987 Biomechanics Symposium, ASME Applied Mechanics, Bioengineering, and Fluids Engineering Conference, pp. 161-164. AMD, Cincinnati, OH.

El-Bohy, A., Cavanaugh, J.M., Getchell, M.L., Bulas, T., Getchell, T.V., and King, A.I. (1988) Localization of substance P and neurofilament immunoreactive fibers in the lumbar facet joint capsule and supraspinous ligament of the rabbit. Brain Research 460(2): 379-382.

Freeman, M.D., Croft, A.C., Rossignol, A.M., Weaver, D.S., and Reiser M. (1999) A review and methodologic critique of the literature refuting whiplash syndrome. Spine 24(1): 86-96.

Giles, L.G., and Harvey, A.R. (1987) Immunohistochemical demonstration of nociceptors in the capsule and synovial folds of human zygapophyseal joints. British Journal of Rheumatology 26(5): 362-364.

Gilmore, S.A., and Sims, T.J. (1997) Glial-glial and glial-neuronal interfaces in radiation-induced, glia-depleted spinal cord. Journal of Anatomy 190(1): 5-21.

Grauer, J.N., Panjabi, M.M., Cholewicki, J., Nibu, K., and Dvorak, J. (1997) Whiplash produces an S-shaped curvature of the neck with hyperextension at lower levels. Spine 22(21): 2489-2494.

Guyton, A.C., and Hall, J.E. (1996) Textbook of Medical Physiology. W.B. Saunders Company, Philadelphia, PA.

Hashizume, J., DeLeo, J.A., Colburn, R.W., and Weinstein, J.N. (2000) Spinal glial activation and cytokine expression after lumbar root injury in the rat. Spine 25(10): 1206-1217.

Hill-Felberg, S.J., McIntosh, T.K., Oliver, D.L., Raghupathi, R., and Barbarese, E. (1999) Concurrent loss and proliferation of astrocytes following lateral fluid percussion brain injury in the adult rat. Journal of Neuroscience Research 57(2): 271-279.

Hoffman, A.H., and Grigg, P. (1984) A method for measuring strains in soft tissue. Journal of Biomechanics 17(10): 795-800.

Hubbard, R.D., Lee, K.L., and Winkelstein, B.A. (2003) Effects of nerve root compression magnitude on behavioral outcomes: preliminary findings in a neck pain model. National Neurotrauma Society Meeting, #P340. Biloxi, MS.

Hubbard, R.D., Rothman, S.M., and Winkelstein, B.A. (2004) Mechanisms of persistent neck pain following nerve root compression injury: understanding behavioral hypersensitivity in the context of spinal cytokine responses and tissue biomechanics. North American Spine Society 19th Annual Meeting. Chicago, IL.

Ianuzzi, A., Little, J.S., Chiu, J.B., Baitner, A., Kawchuk, G., and Khalsa, P.S. (2004) Human lumbar facet joint capsule strains: I. During physiological motions. The Spine Journal 4: 141-152.

Inami, S., Shiga, T., Tsujino, A., Yabuki, T., Okado, N., and Ochiai, N. (2001) Immunohistochemical demonstration of nerve fibers in the synovial fold of the human cervical facet joint. Journal of Orthopaedic Research 19: 593-596.

Ito, S., Ivancic, P.C., Panjabi, M.M., and Cunningham, B.W. (2004) Soft tissue injury threshold during simulated whiplash. Spine 29(9): 979-987.

Ji, R.R., and Woolf, C.J. (2001) Neuronal plasticity and signal transduction in nociceptive neurons: implications for the initiation and maintenance of pathological pain. Neurobiology of Disease 8: 1-10.

Kallakuri, S., Singh, A., Chen, C., and Cavanaugh, J.M. (2004) Demonstration of substance P, calcitonin-gene-related peptide, and protein gene product 9.5 containing nerve fibers in human cervical facet joint capsules. Spine 29(11) 1182-1186.

Kandel, E.R., Schwartz, J.H., and Jessell, T.M. (2000) Principles of Neural Science. McGraw-Hill, New York.

Kaneoka, K., Ono, K., Inami, S., and Hayashi, K. (1999) Motion analysis of cervical vertebrae during whiplash loading. Spine 24(8): 763-770.

Khalsa, P.S., Hoffman, A.H., and Grigg, P. (1996) Mechanical states encoded by stretch-sensitive neurons in feline joint capsule. Journal of Neurophysiology 76(1): 175-187.

Kim, S.H., and Chung, J.M. (1992) An experimental model for peripheral neuropathy produced by segmental spinal nerve ligation in the rat. Pain 50(3): 355-363.

Kivioja, J., Rinaldi, L., Ozenci, V., Kouwenhoven, M., Kostulas, N., Lindgren, U., and Link, H. (2001) Chemokines and their receptors in whiplash injury: elevated RANTES and CCR-5. Journal of Clinical Immunology 21(4): 272-277.

Lai, W.M., Rubin, D., and Krempl, E. (1993) Introduction to Continuum Mechanics. Pergamon Press, Tarrytown, NY.

Lee, K.E., Thinnes, J.H., Gokhin, D.S., Winkelstein, B.A. (2004) A novel rodent neck pain model of facet-mediated behavioral hypersensitivity: Implications for persistent pain and whiplash injury. Journal of Neuroscience Methods 137(2): 151-159.

Liu, L., Rudin, M., Kozlova, E.N. (2000) Glial cell proliferation in the spinal cord after dorsal rhizotomy or sciatic nerve transection in the adult rat. Experimental Brain Research 131(1): 64-73.

Lord, S.M., Barnsley, L., Wallis, B.J., and Bogduk, B. (1996) Chronic cervical zygapophysial joint pain after whiplash. Spine 21(15): 1737-1745.

Luan, F., Yang, K.H., Deng, B., Begeman, P.C., Tashman, S., and King, A.I. (2000) Qualitative analysis of neck kinematics during low-speed rear-end impact. Clinical Biomechanics 15: 649-657.

McLain, R.F. (1994) Mechanoreceptor endings in human cervical facet joints. Spine 19(5): 495-501.

Meon, V.K., and Landerholm, T.E. (1994) Intralesion injection of basic fibroblast growth factor alters glial reactivity to neural trauma. Experimental Neurology 129(1): 142-154.

Merskey, H. and Bogduk, N. (1994) Classification of Chronic Pain, Second Edition, IASP Task Force on Taxonomy. IASP Press, Seattle.

Obata, K., Yamanaka, H., Fukuoka, T., Yi, D., Tokunaga, A., Hashimoto, N., Yoshikawa, H., and Noguchi, K. (2003) Contribution of injured and uninjured dorsal root ganglion neurons to pain behavior and the changes in gene expression following chronic constriction injury of the sciatic nerve in rats. Pain 101: 65-77.

Ochoa, J.L. (2003) Quantifying sensation: "Look back in allodynia". European Journal of Pain 7: 369-374.

Ohtori, S., Takahashi, K., and Moriya, H. (2003) Calcitonin gene-related peptide immunoreactive DRG neurons innervating the cervical facet joints show phenotypic switch in cervical facet injury in rats.

Olmarker, K., Storkson, R., Berge, O.G. (2002) Pathogenesis of sciatic pain: a study of spontaneous behavior in rats exposed to experimental disc herniation. Spine 27(12): 1312-1317.

Ono, K., Kaneoka, K., Wittek, A., and Kajzer, J. (1997) Cervical injury mechanism based on the analysis of human cervical vertebral motion and head-neck-torso kinematics during low speed rear impacts. Proc. 41st Stapp Car Crash Conference, pp. 339-356. Society of Automotive Engineers, Warrendale, PA.

Panjabi, M.M., Pearson, A.M., Ito, S., Ivancic, P.C., and Wang, J.-L. (1998a) Cervical spine curvature during simulated whiplash. Clinical Biomechanics 19: 1-9.

Panjabi, M.M., Cholewicki, J., Nibu, K., Grauer, J.N., and Vahldiek, M. (1998b) Capsular ligament stretches during in vitro whiplash simulations. Journal of Spinal Disorders 11: 227-232.

Panjabi, M.M., Pearson, A.M., Ito, S., Ivancic, P., and Wang, J.-L. (2004) Cervical spine curvature during simulated whiplash. Clinical Biomechanics 19: 1-9.

Pearson, A.M., Ivancic, P.C., Ito, S., and Panjabi, M.M. (2004) Facet joint kinematics and injury mechanisms during simulated whiplash. Spine 29(4): 390-397.

Pickar, J.G., and McLain, R.F. (1995) Responses of mechanosensitive afferents to manipulation of the lumbar facet in the cat. Spine 20(22): 2379-2385.

Piehl, F., and Lidman,O. (2001) Neuroinflammation in the rat—CNS cells and their role in the regulation of immune reactions. Immunological Reviews 184: 212-225.

Pintar, F.A., Yoganandan, N., Myers, T. Elhagedib, A., and Sances, A. (1992) Biomechanical properties of human lumbar spine ligaments. Journal of Biomechanics 25(11): 1351-1356.

Quinlan, K.P., Annest, J.L., Myers, B., Ryan, G., and Hill, H. (2004) Neck strains and sprains among motor vehicle occupants—United States, 2000. Accident Analysis and Prevention 36: 21-27.

Rutkowski, M.D., Winkelstein, B.A., Hickey, W.F., Pahl, J.L., and DeLeo, J.A. (2002) Lumbar nerve root injury induces central nervous system neuroimmune activation and neuroinflammation in the rat: relationship to painful radiculopathy. Spine 27(15): 1604-1613.

Sheather-Reid, R.B., and Cohen, M.L. (1998) Psychophysical evidence for a neuropathic component of chronic neck pain. Pain 75: 341-347.

Siegmund, G.P., Myers, B.S., Davis, M.B., Bohnet, H.F., and Winkelstein, B.A. (2001) Mechanical evidence of cervical facet capsule injury during whiplash. Spine 26(19): 2095-2101.

Smit, T.H. (2002) The use of a quadruped as an in vivo model for the study of the spine-biomechanical considerations. European Spine Journal 11: 137-144.

Sterling, M., Jull, G., Vicenzino, B., and Kenardy, J. (2003) Sensory hypersensitivity occurs soon after whiplash injury and is associated with poor recovery. Pain 104: 509-517.

Sweitzer, S.M., Hickey, W.F., Rutkowski, M.D., Pahl, J.L., and DeLeo, J.A. (2002) Focal peripheral nerve injury induces leukocyte trafficking into the central nervous system: potential relationship to neuropathic pain. Pain 100(1-2): 163-170.

Takahashi, Y., and Nakajima, Y. (1996) Dermatomes in the rat limbs as determined by antidromic stimulation of sensory C-fibers in spinal nerves. Pain 67: 197-202.

Vijayan, V.K., Lee, Y.L., and Eng, L.F. (1990) Increase in glial fibrillary acidic protein following neural trauma. Molecular and Chemical Neuropathy. 13(1-2): 107-118.

Wang, H., Sun, H., Della Penna, K., Benz, R.J., Xu, J., Gerhold, D.L., Holder, D.J., and Koblan, K.S. (2002) Chronic neuropathic pain is accompanied by global changes in gene expression and shares pathobiology with neurodegenerative states. Neuroscience 114(3): 529-546.

Watkins, L.R., Maier, S.F., and Goehler, L.G. (1995) Immune activation: the role of pro-inflammatory cytokines in inflammation, illness responses and pathological pain states. Pain 63: 289-302.

Watkins, L.R., Milligan, E.D., and Maier, S.F. (2001) Spinal cord glia: new players in pain. Pain 93: 201-205.

Winkelstein, B.A. (1999) A mechanical basis for whiplash injury: the cervical facet joint, spinal motion segment, and combined loading. Ph.D. Thesis, Duke University.

Winkelstein, B.A., Nightingale, R.W., Richardson, W.J., and Myers, B.S. (1999) Cervical facet joint mechanics: its application to whiplash injury. Proc. 43rd Stapp Car Crash Conference, pp. 243-252. Society of Automotive Engineers, Warrendale, PA.

Winkelstein, B.A., Nightingale, R.W., Richardson, W.J., and Myers, B.S. (2000) The cervical facet capsule and its role in whiplash injury. Spine 25(10): 1238-1246.

Winkelstein, B.A., Rutkowski, M.D., Sweitzer, S.M., Pahl, J.A., and DeLeo, J.A. (2001a) Nerve injury proximal or distal to the DRG induces similar spinal glial activation and selective cytokine expression but differential behavioral responses to pharmacologic treatment. The Journal of Comparative Neurology 439: 127-139.

Winkelstein, B.A., Rutkowski, M.D., Weinstein, J.N., and DeLeo, J.A. (2001b) Quantification of neural tissue injury in a rat radiculopathy model: comparison of local deformation, behavioral outcomes, and spinal cytokine mRNA for two surgeons. Journal of Neuroscience Methods 111: 49-57.

Winkelstein, B.A., and DeLeo, J.A. (2002) Nerve root injury severity differentially modulates spinal glial activation in a rat lumbar radiculopathy model: considerations for persistent pain. Brain Research 956: 294-301.

Winkelstein, B.A., Hubbard, R.D., and DeLeo, J.A. (2003) Biomechanics and painful injuries: tissue & CNS responses for nerve root mechanical injuries. International Mechanical Engineering Congress & Exposition #43117. ASME, Washington, D.C.

Yamashita, T., Cavanaugh, J.M., El-Bohy, A.A., Getchell, T.V., and King, A.I. (1990) Mechanosensitive afferent units in the lumbar facet joint. Journal of Bone & Joint Surgery 72(6): 865-870.

Yoganandan, N., and Pintar, F.A. (1997) Inertial loading of the human cervical spine. Journal of Biomechanical Engineering 119: 237-240.

Yoganandan, N., Pintar, F.A., and Klienberger, M. (1998) Cervical spine vertebral and facet joint kinematics under whiplash. Journal of Biomechanical Engineering 120: 305-307.

Yoganandan, N., Cusick, J.F., Pintar, F.A., and Rao, R.D. (2001) Whiplash injury determination with conventional spine imaging and cryomicrotomy. Spine 26(22): 2443-2448.

Yoganandan, N., Pintar, F.A., and Cusick, J.F. (2002) Biomechanical analyses of whiplash injuries using an experimental mode. Accident Analysis and Prevention 34: 663-671.

Zhang, J.-M., Song, X.-J., and LaMotte, R.H. (1999) Enhanced excitability of sensory neurons in rats with cutaneous hyperalgesia produced by chronic compression of the dorsal root ganglion. Journal of Neurophysiology 82: 3359-3366.

Zimmermann M. (1983) Ethical guidelines for investigations of experimental pain in conscious animals. Pain 16:109-110.

APPENDIX

Table A1. Summary data of injury mechanics, allodynia, and GFAP staining for individual rats in the behavioral study.

				Allodynia (avg both paws, at day 14)		Average normalized pixel intensity of GFAP staining		
Rat	**Weight (g)**	**Forceps Displacement (x) (mm)**	**Vertebral Distraction (x) (mm)**	**1.4 g**	**2.0 g**	**Lamina I**	**Lamina X**	**White Matter**
K4	294	1.22	0.21	4.5	5.5	13049.96	18946.45	8235.53
5	340	1.65	0.72	1.5	2.5	18471.78	17553.41	8812.15
8	350	1.51	0.53	4	3	14909.13	16743.14	6498.53
17	318	1.36	1.53	2	6.5	9239.23	13162.89	6515.94
18	306	1.33	1.51	4.5	5	11188.39	15865.48	8798.80
20	330	1.19	0.89	4	5	11608.14	16402.03	11204.97
SV Avg (SD)	***323 (21)***	***1.38 (0.18)***	***0.90 (0.53)***	***3.4 (1.3)***	***4.6 (1.5)***	***13077.77 (3253.12)***	***16445.57 (1933.11)***	***7833.62 (1753.31)***
K1	318	0.51	0.14	4	2.5	N/A	N/A	N/A
K7	320	0.52	0.23	3.5	1	11642.81	18912.28	11658.53
K11	296	0.51	0.17	3	3	12467.74	16040.59	9840.59
6	348	0.81	0.28	0.5	3	11957.71	12736.77	5689.46
11	366	0.63	0.12	0.5	1.5	6939.65	9276.60	4836.22
21	326	0.44	0.20	1	1	4103.36	10410.43	5803.40
PV Avg (SD)	***329 (25)***	***0.57 (0.13)***	***0.19 (0.06)***	***2.1 (1.6)***	***2.0 (1.0)***	***9422.25 (3711.07)***	***13475.33 (3990.91)***	***7565.64 (3000.10)***
K6	310	--	--	4.5	2.5	11907.63	18449.53	11236.53
K15	330	--	--	2.5	1	5619.47	12421.52	9522.67
K16	332	--	--	2.5	2.5	6747.77	11601.74	7583.65
9	358	--	--	0.5	1	10879.75	12302.06	6825.65
22	318	--	--	0.5	1	5763.40	11680.86	4731.12
23	252	--	--	1	0.5	7706.45	15199.93	7102.15
Sham Avg (SD)	***317 (36)***	--	--	***1.9 (1.6)***	***1.4 (0.9)***	***8104.08 (2676.61)***	***13609.27 (2713.92)***	***7833.62 (2265.91)***

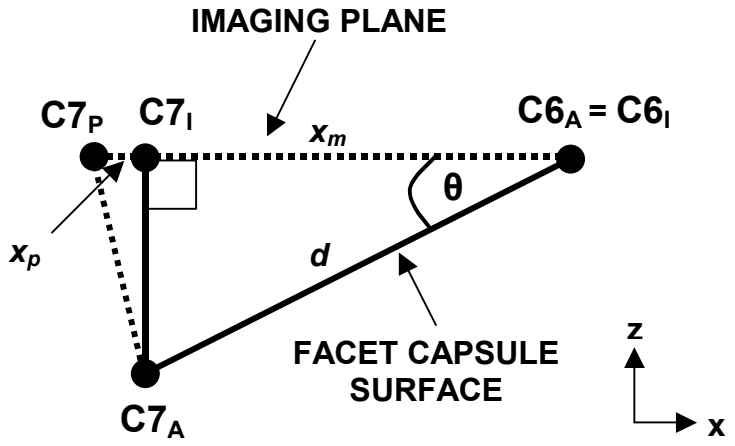

Figure A1. Schematic showing the x-coordinate projection method for C7 capsule marker positions, which accounts for the inclination (θ) of the rat facet capsule in the caudal-rostral (x) direction. This *lateral* view depicts the *actual* facet capsule surface as the plane containing C6 and C7 capsule markers ($C6_A$ & $C7_A$). However, 2D imaging projects the capsule markers into a horizontal plane and the capsule marker centroids are imaged at points $C6_I$ (same as $C6_A$) and $C7_I$. To accommodate for the discrepancy between the actual capsule surface and 2D imaging effects, *actual* caudal markers are mathematically projected into the imaging plane using the capsule inclination angle (θ) (see calculations below). Briefly, the actual distance between the capsule markers (d) is calculated by dividing the measured distance (x_m) (from imaging) between the markers by the cosine of the angle of capsule inclination (θ=52±2.6°). The actual marker position ($C7_A$) in x is projected onto the imaging plane ($C7_P$) such that the sum of the distance between the imaged and projected C7 markers (x_p), and the distance between the C6 and C7 markers as measured by the camera (x_m), is equivalent to the actual distance between the C6 and C7 markers (d).

PROJECTION CALCULATION

Using the angle of facet inclination (θ) and the distance between imaged marker locations (x_m), the distance, d, between the actual capsule markers $C6_A$ and $C7_A$, is estimated using trigonometric relationships in the x-z plane:

$$d = \frac{x_m}{\cos\theta}, \tag{A1}$$

where x_m is the measured distance, in x, of the imaging plane, between capsule markers $C6_I$ (same as $C6_A$) and $C7_I$. Θ is the angle of inclination, in degrees, between the capsule surface and the horizontal (x=0).

For θ=52.2° (as determined in the capsule topography study of the rat C6/C7 facet capsule),

$$d = \frac{x_m}{0.61} = 1.63(x_m). \tag{A2}$$

With d determined, the point $C7_I$ is projected to $C7_P$, by the amount, x_p, according to:

$$x_p = d - x_m, \tag{A3}$$

For strain analysis, this projection value, x_p, is added to the x-coordinate of $C7_I$ to create $C7_P$, a marker for which the x-coordinate is corrected, accounting for the inclination of the facet capsule surface. The actual C6 marker ($C6_A$) and projected C7 marker ($C7_P$) are used in all subsequent calculations of capsule strain.